Articles

A Zinc Ribbon Protein in DNA Replication: Primer Synthesis and Macromolecular Interactions by the Bacteriophage T4 Primase†

Ann M. Valentine,‡ Faoud T. Ishmael,§ Vincent K. Shier,‡ and Stephen J. Benkovic*,‡

Department of Chemistry, The Pennsylvania State University, 415 Wartik Laboratory, University Park, Pennsylvania 16802, and Department of Biochemistry and Molecular Biology, The Pennsylvania State University College of Medicine, 500 University Drive, Hershey, Pennsylvania 17033

Received April 26, 2001; Revised Manuscript Received September 26, 2001

ABSTRACT: The gene product 61 primase protein from bacteriophage T4 was expressed as an intein fusion and purified to homogeneity. The primase binds one zinc ion, which is coordinated by four cysteine residues to form a zinc ribbon motif. Factors that influence the rate of priming were investigated, and a physiologically relevant priming rate of ∼1 primer per second per primosome was achieved. Primase binding to the single-stranded binding protein (1 primase:4 gp32 monomers; K_d ∼ 860 nM) and to the helicase protein in the presence of DNA and ATP-γ-S (1 primase:1 helicase monomer; K_d ∼ 100 nM) was investigated by isothermal titration calorimetry (ITC). Because the helicase is hexameric, the inferred stoichiometry of primase binding as part of the primosome is helicase hexamer:primase in a ratio of 1:6, suggesting that the active primase, like the helicase, might have a ring-like structure. The primase is a monomer in solution but binds to single-stranded DNA (ssDNA) primarily as a trimer (K_d ∼ 50−100 nM) as demonstrated by ITC and chemical cross-linking. Magnesium is required for primase−ssDNA binding. The minimum length of ssDNA required for stable binding is 22−24 bases, although cross-linking reveals transient interactions on oligonucleotides as short as 8 bases. The association is endothermic at physiologically relevant temperatures, which suggests an overall gain in entropy upon binding. Some possible sources of this gain in entropy are discussed.

DNA replication, one of the fundamental processes of the cell, must occur with stringent control to avoid deleterious mutations and damage to genetic material. A DNA copy must be made rapidly enough to keep pace with cell division. One system in which DNA replication has been studied in elegant detail is the bacteriophage T4 (*1*, *2*). DNA is replicated as it unwinds (Figure 1) in a process requiring the coordinated action of multiple proteins. A helicase protein (gene product 41 or gp41)[1] encircles the lagging strand and, with translocation driven by ATP hydrolysis, unwinds the DNA. Loading of the helicase is facilitated by a helicase accessory factor (gp59). On the leading strand, a polymerase holoenzyme comprising several proteins synthesizes the complement in a processive manner. The polymerase (gp43) is held onto the DNA by a trimeric clamp protein (gp45), which circumscribes the DNA. A clamp loader (gp44/62) facilitates gp45 loading.

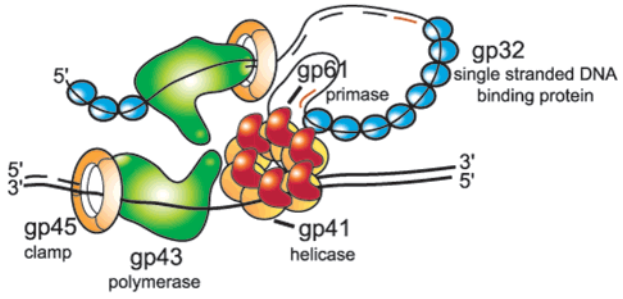

FIGURE 1: An active T4 replication fork. Double-stranded DNA is unwound by the gp41 helicase as it is copied on leading and lagging strands by the gp43 polymerase, which is made processive by the gp45 trimeric clamp. Meanwhile, exposed single-stranded DNA is protected by the gp32 single-stranded DNA binding protein, and priming is catalyzed by the gp61 primase. The clamp loading (gp44/62) and helicase loading (gp59) proteins are not shown.

The polymerase can only function in the 5′ to 3′ direction, so the lagging strand copy must be synthesized discontinu-

† This work was supported by National Institutes of Health Grants GM13306 (S.J.B.), GM20154 (A.M.V.), and DK19691 (F.T.I.).

‡ Department of Chemistry, The Pennsylvania State University.

§ Department of Biochemistry and Molecular Biology, The Pennsylvania State University College of Medicine.

[1] Abbreviations: gp32, single-stranded DNA binding protein; gp41, helicase; gp43, DNA polymerase; gp44/62, clamp loader; gp45, processivity clamp for the DNA polymerase; gp59, helicase loading protein; gp61, DNA-dependent RNA polymerase or primase; Tris, tris(hydroxymethyl)aminomethane; HEPES, *N*-(2-hydroxyethyl)piperazine-*N*′-2-ethanesulfonic acid; β-ME, β-mercaptoethanol; DTNB, 5,5′-dithiobis(2-nitrobenzoic acid); ATP-γ-S, adenosine 5′-*O*-(3-thiotriphosphate); BMH, 1,6-bismaleimidohexane; Ru(II)bpy$_3^{2+}$, tris(2,2′-bipyridyl)dichlororuthenium(II) hexahydrate; ITC, isothermal titration calorimetry; ssDNA, single-stranded DNA; dsDNA, double-stranded DNA.

10.1021/bi0108554 CCC: $20.00
Published on Web 11/21/2001

ously as the template is exposed by the helicase. As DNA is unwound, the resulting single-stranded DNA (ssDNA) is stabilized by a ssDNA binding protein (gp32). A second polymerase holoenzyme functions on the lagging strand and requires a primer for extension. This primer is made by a primase protein (gp61), which assembles with the helicase to form the primosome. The primase synthesizes pentaribonucleotides repeatedly on the lagging strand, and the polymerase extends them into stretches of oligonucleotides known as Okazaki fragments. Later, the pentaribonucleotides are removed, and ligase enzymes join the Okazaki fragments to produce a continuous complementary strand. Much is known about the polymerase holoenzyme in bacteriophage T4 and its protein components (*3*), but comparatively little is known about the primosome.

The primase is a 40 kDa protein made up of three domains. The N-terminal domain contains a zinc binding domain known as a zinc ribbon, although until the current work zinc binding had not been demonstrated for the T4 primase. The structure of this domain in the primase from *Bacillus stearothermophilus* was recently reported (*4*). Zinc ribbon motifs also occur in other proteins that bind DNA such as replication and repair proteins as well as in transcription factors. NMR structures of these motifs from several proteins are available (*5*−*8*). When the protein encounters a recognition site (in bacteriophage T4, 5′-GTT-3′ in vivo or in vitro and 5′-GCT-3′ in vitro when cytosines are not hydroxymethylated as they are in T4 DNA), it makes a complementary pentaribonucleotide in the 5′ to 3′ direction. Although the 3′ T is required for recognition, it is not copied into the resulting primer. The primers therefore have the sequence 5′-ACNNN-3′ for priming at 5′-GTT-3′ sites and 5′-GCNNN-3′ for priming at 5′-GCT-3′ sites (*9*, *10*). Primases from *E. coli* and bacteriophage T7 have similar zinc ribbon sequences but recognize different priming sites and produce primers of different length (*11*). When the zinc ribbon sequence from T7 was replaced with those from *E. coli* and bacteriophage T4, the resulting chimeric proteins were active but primed at sequences different than either of their parent proteins (*12*). This result strongly suggests that some, but not all, of the priming site recognition is afforded by the zinc ribbon motif.

The middle domain of the primase is the catalytic domain, responsible for ribonucleotide polymerization. The structure of a homologous domain for the enzyme from *E. coli* was recently reported (*13*, *14*). Many of the proteins involved in DNA replication are conserved in both structure and function among prokaryotes and eukaryotes. After consideration of their sequence, however, and before structures were available, Koonin and co-workers related the catalytic domain of the prokaryotic primases to bacterial topoisomerases rather than to eukaryotic primases (*15*, *16*). These DnaG-type primases (after the protein designation in *E. coli*) were predicted to have a TOPRIM fold, confirmed by subsequent X-ray crystallographic studies (*13*, *14*). The structure of the replicative primase from an archeon, on the other hand, is unrelated in fold to the DnaG-type primases (*17*). Although the structures of the several types of primases differ, they are likely to share common characteristics of function. The C-terminal domain of the T4 primase is involved in protein−protein interactions with the helicase (*18*), and no structure is known.

Table 1: Primers Used in This Study (5′ to 3′)

oligo	sequence
61forI	GCGGAATTCCATATGTCATCAATACCTTGGATT
61revI	GCGGAATTCGCTCTTCCGCAAATCTTAGCATAT-TTAGATAG
61qcfor	GCTATCTAAATATGCTAAGGGTTGCGGAAGAG-CGAATCG
61qcrev	CGATTCGCTCTTCCGCAACCCTTAGCATATTT-AGATAGC

The goal of this work was to determine conditions under which priming occurs at a physiologically relevant rate. To this end, the binding of primase with helicase (gp41), accessory protein (gp59), and single-stranded DNA binding protein (gp32) was investigated as well as the interaction of the primase with nonspecific and specific DNA sequences. The investigations necessitated an improved preparation of the enzyme which was achieved through intein fusion and affinity column purification. These studies revealed unexpected stoichiometries of various primase complexes directing us toward conditions that gave priming at rates reaching those demanded by an active replisome.

EXPERIMENTAL PROCEDURES

Cloning of the Primase. The primase protein was cloned from T4 genomic DNA (Sigma) by using the primers 61forI and 61revI shown in Table 1. These primers have *Eco*RI restriction sites used for subcloning in pUC flanking *Nde*I and *Sap*I restriction sites for insertion into a homemade pET-IMPACT plasmid (New England Biolabs) (*19*). The amplified insert was purified by agarose gel electrophoresis, digested with *Eco*RI, and ligated into pUC19 which had also been digested with *Eco*RI. The ligation mixture was used to electrotransform *E. coli* DH5α cells, and positives were selected by their ability to grow on LB plates supplemented with ampicillin. A 50 mL culture in LB/ampicillin was grown from a single colony, and the plasmid (pUCgp61) was isolated by midiprep (Qiagen). The pUCgp61 plasmid and a pET-IMPACT plasmid were digested with *Sap*I for 3 h at 37 °C. *Nde*I was added to the pUCgp61 digest, and both *Nde*I and shrimp alkaline phosphatase were added to the pET-IMPACT plasmid digest. The digestion was allowed to continue for 10 h. The resulting insert and digested plasmid were agarose gel purified and ligated. The ligation mixture was used to transform *E. coli* DH5α cells, and the plasmid (pET61I) was isolated by midiprep from a 50 mL culture. The presence and sequence of the insert were verified by DNA sequencing (Pennsylvania State University Nucleic Acid Facility). Compared to the published sequence (NP_049648 in the NCBI database), there is a single nucleotide change from G to A at the codon for amino acid 211. This change results in a lysine residue at position 211 rather than glutamate, which is predicted in the database sequence. The same sequence was found after three separate amplifications from T4 genomic DNA, and was confirmed as the correct sequence (Nancy Nossal, personal communication).

The native protein sequence exhibited a poor intein cleavage yield during purification (see below), and so the C-terminal amino acid was changed from isoleucine to glycine (I342G) to improve this yield. The pUCgp61 plasmid was mutated by using the Quikchange protocol (Stratagene) and primers 61qcfor and 61qcrev in Table 1. The mutated

insert was excised and ligated into the pET-IMPACT plasmid as described above to produce plasmid pET61I342G. The presence of the mutation and the absence of undesired mutations were confimed by sequencing. The purified protein had the same activity as wild type and exhibited identical zinc and DNA binding properties.

Protein Purification. E. coli BL21(DE3) cells were electrotransformed with plasmid p61I342G. Transformants were selected with 50 μg/mL kanamycin on LB agar plates. A single colony was used to inoculate a 5 mL culture in LB media supplemented with kanamycin (50 μg/mL), which was grown at 37 °C for 12 h. A 50 mL culture in the same media was inoculated with 0.5 mL of this material, and was grown to $OD_{600} = 0.5$. This culture was used to inoculate a 20 L fermenter. After 8 h of growth at 37 °C ($OD_{600} \sim 10$), the temperature was reduced to 18 °C. Protein expression was induced by the addition of IPTG (0.1 mM), and induction proceeded for 10 h. The cells (~1 kg) were then harvested and stored at −80 °C.

All protein purification steps were performed at 4 °C. Cell paste (150 g) was thawed in 250 mL of column buffer [20 mM Tris (pH 8), 0.1 mM EDTA, and 10% glycerol] with 200 mM NaCl. Cells were lysed by sonication, and cell-free extract was produced by centrifugation for 1 h at 6000*g* followed by ultracentrifugation of the resulting supernatant (60000*g*) for 30 min. The cell-free extract was loaded at 1 mL/min on a chitin column (New England Biolabs) (~25 mL bed volume) equilibrated in column buffer with 200 mM NaCl. The column was washed at 1 mL/min with 800 mL of column buffer with 1 M NaCl and then 75 mL of column buffer with 200 mM NaCl. The column was then flushed with 40 mL of the latter buffer containing 75 mM β-mercaptoethanol (β-ME). The column was closed off and cleavage allowed to proceed at 4 °C for 24 h.

The cleaved protein was eluted from the column with column buffer containing 200 mM NaCl. Fractions containing protein (~50 mL) as judged by SDS−PAGE were pooled and loaded at 0.5 mL/min onto a P11 phosphocellulose column (Whatman) (~12 mL bed volume) equilibrated in column buffer with 200 mM NaCl and 10 mM β-ME. The column was washed with 50 mL of the same buffer, and protein was eluted at 0.7 mL/min by using a gradient from 200 to 600 mM NaCl in 400 mL total volume. Fractions containing primase protein as judged by SDS−PAGE were pooled and concentrated to approximately 100 μM by using an Amicon stirred cell concentrator equipped with a YM30 membrane. Protein concentration was determined by using an extinction coefficient of $\epsilon_{280\ nm} = 70\ 000\ M^{-1}\ cm^{-1}$ (*20*). A typical preparation yielded approximately 60−75 mg of purified protein at >98% purity (Figure S1).

Single-stranded binding protein was purified from a pET-IMPACT plasmid constructed by Dr. Stephen Alley according to the same procedure described for the primase above. Helicase protein and gp59 protein were a gift from Dr. M. Uljana Mayer.

Zinc Analysis. Protein was dialyzed against four changes of 4 L of chelex-treated column buffer without glycerol and with 50 mM NaCl and 10 mM β-ME. Atomic absorption analysis was carried out in flame mode by using a Perkin-Elmer 730 Atomic Absorption Spectrophotometer at the Pennsylvania State University Materials Characterization Lab.

Table 2: Primase Binding to and Priming on Oligos of Varying Length

oligo	sequence	N^a	K_d (nM)	priming?
8mer	5′-GAG**GTT**TG-3′	*b*	*b*	no
15mer	5′-CGGGAG**GTT**TGCATG-3′	*b*	*b*	no
20mer	5′-GGAGGGAG**GTT**TGCA-ACTGA-3′	*b*	*b*	no
22mer	5′-GGGAGGGAG**GTT**TGC-AACTGAT-3′	3 ± 1	330	no
24mer	5′-TGGGAGGGAG**GTT**TGC-AACTGATC-3′	4 ± 1	53	no
45mer	5′-GGGTGGGAGGGAG**GTT**-TGCAACTGATCGATGAT-AGTACGTCTGTG-3′	4 ± 1	40	yes

[a] Moles of primase binding per mole of ssDNA. [b] No binding observed.

Determination of Free Thiol. DTNB titrations were carried out as described in the literature (*21*).

Primase Activity Assays. Activity assays were performed essentially as reported earlier (*22*), by monitoring the formation of radiolabeled pentaribonucleotides after electrophoretic separation. In a typical experiment, 125 nM helicase hexamers, 750 nM primase, 750 nM gp59, 6 μM gp32, 1 mM rNTPs including [α-^{32}P]CTP (New England Nuclear), 4 mM additional ATP, and single-stranded nucleotide template [500 ng of M13mp18 DNA (Bayou Biolabs) or 1 μM oligonucleotide (Table 2)] were incubated at 37 °C in a total reaction volume of 40 μL in a buffer containing 25 mM Tris (pH 7.5), 150 mM KOAc, 10 mM $Mg(OAc)_2$, and 10 mM β-ME. At various times, 10 μL aliquots were quenched in an equal volume of 1 N HCl and extracted with 20 μL of phenol/chloroform, and the aqueous layer was neutralized with 2.2 μL of 3 M NaOH in 1 M Tris base. A 10 μL aliquot of the resulting aqueous layer was added to 10 μL of gel loading dye. It was observed that bromophenol blue in the loading dye bound to the pentaribonucleotides (*23*) and caused them to run aberrantly, so this dye was omitted from the solution and only xylene cyanol was used as a marker. Oligoribonucleotides were separated by 20% denaturing gel electrophoresis followed by analysis by phosphorimaging techniques. A typical result is shown in Figure S2. The calibrated specific activity of the radiation was used to convert counts of radiation to moles of CTP incorporated. Primers have the sequences 5′-ACNNN-3′ and 5′-GCNNN-3′, so were assumed to have an average of 1.75 mol of CTP per mole of primer.

Oligonucleotide Synthesis and Purification. Oligonucleotides were synthesized on a 1 μmol scale by using an Expedite 8909 DNA synthesizer according to the manufacturers' instructions. Oligos were purified by 20% denaturing polyacrylamide Hoefer gels and isolated by crush and soak (*24*) followed by Sep-Pak (Waters). Oligos were 5′ end-labeled with ^{32}P by using polynucleotide kinase (USB) and separated by denaturing polyacrylamide to ascertain purity.

Isothermal Titration Calorimetry. Binding of various macromolecules was assessed by isothermal titration calorimetry on a thermostated MicroCal VP-ITC system. Proteins of interest were dialyzed into complex buffer [20 mM HEPES or Tris, pH 7.5, 150 mM KOAc, 10 mM $Mg(OAc)_2$] for at least 8 h to achieve dialysis equilibrium. Protein solutions were then centrifuged to remove particles before

beginning the experiment. Oligonucleotides dissolved in water were diluted directly into complex buffer if the added volume would comprise less than 1% of the final volume. Otherwise, oligonucleotide solutions were dried on a Speedvac and the oligos redissolved in complex buffer. Protein and DNA solutions were quantitated by UV/Vis absorbance. All solutions were degassed prior to use. This degassing step was determined in control experiments not to affect protein activity.

There are several recent reviews of isothermal titration calorimetry and data fitting (*25*−*29*). Data were analyzed by Origin 5.0 (MicroCal). Heats of dilution were subtracted from all data before fitting. Each dilution heat was determined in an independent control experiment by injecting the macromolecule into buffer. These heats were much smaller than the heats of binding. Data analysis requires a binding model, and fitting returns values for the binding constant K, ΔH of binding, ΔS of binding, and the binding stoichiometry N as described below.

In the simplest case of the binding of ligand (L) to protein (P) with 1:1 stoichiometry:

$$P + L \leftrightarrow PL \quad (1)$$

and since $[P]_t = [P] + [PL]$, the concentration of PL complex is

$$[PL] = [P]_t\{K[L]/(1 + K[L])\} \quad (2)$$

where K is the associative binding constant and $[P]_t$ is the total protein concentration. In the binding experiment, the heat absorbed or produced (q) is a product of the concentration of the bound ligand, the cell volume V, and the molar binding enthalpy ΔH:

$$q = V\Delta H[P]_t\{K[L]/(1 + K[L])\} \quad (3)$$

In the one-site binding model employed for most of the studies described in this paper, each protein is considered to have a finite number of identical noninteracting binding sites. The total heat absorbed or produced becomes

$$q = NV\Delta H[PL_n] \quad (4)$$

where N is the number of sites per molecule of protein. The measured value of q is thus dependent on the values of the independent variables ΔH, K, and N. These are obtained by fitting binding simulations for q after each injection throughout the entire titration using the following equation:

$$q = N[P]_t\Delta H(V/2)\cdot\{X - (X^2 - \sqrt{4[L]_t/N[P]_t})\} \quad (5)$$

where $X = \{1 + [L]_t/N[P]_t) + (1/NK[P]_t)\}$.

An initial estimation of these variables is followed by calculation of the change in q after each injection based on these estimates, and comparison of the resulting q values to the experiment. Marquardt algorithms reassign the values of the parameters based on the result of the previous round, and interations continue until the fit is no longer improved. The values of the independent variables are reported as a least-squares fit with statistical error. If the one-site model does not adequately describe the data, more complicated models involving more than one kind of binding site or cooperativity may be invoked.

Analytical Ultracentrifugation. Equilibrium and sedimentation velocity experiments were performed on a Beckman XL-I Analytical Ultracentrifuge in the absorbance mode. Data were acquired by using the XL-I acquisition software. Experiments were performed at 25 °C in complex buffer (see above) or in 50 mM potassium phosphate (pH 8) with 150 mM KCl. Proteins were dialyzed against buffer for at least 12 h at 4 °C before analysis.

For equilibrium experiments, a six-channel centerpiece was employed while several wavelengths were monitored depending on protein concentration so that the total absorbance was between 0.2 and 1 absorbance unit. Data were obtained at speeds of 14 000, 18 000, 24 000, 30 000, and 36 000 rpm. When two consecutive scans taken 2 h apart were completely superimposable, equilibrium was considered to be reached. Data editing was performed with the Origin 3.78 software package (Microcal). Local and global nonlinear least-squares analyses were applied using the program WinNonlinLR 1.05 to extract solution molecular weights.

For sedimentation velocity experiments, two-channel centerpieces were employed to analyze protein samples over a concentration range from 1 to 15 μM at a rotor speed of 36 000 rpm. The data were analyzed by using the transport method and the second moment method available in the Microcal Origin software package to determine the sedimentation coefficient ($s_{25,b}$) at each concentration. The van Holde−Weischet method in the UltraScan II software package was used to verify the sedimentation coefficients. $s^o_{20,w}$ was determined by plotting $s_{25,b}$ against protein concentration, extrapolating to infinite dilution, and then converting the resulting $s^o_{25,b}$ to $s^o_{20,w}$ by using the following equation:

$$s^o_{20,w} = s^o_{T,b}\frac{(1 - \bar{\nu}\rho)_{20,w}(\eta_{T,b})}{(1 - \bar{\nu}\rho)_{T,b}(\eta_{20,w})} \quad (6)$$

where $\bar{\nu}_{25}$ (the partial specific volume of the primase at 25 °C) is 0.7427 mL/g, $\bar{\nu}_{20}$ is 0.7406 mL/g, $\rho_{20,w}$ (the density of water at 20 °C) is 0.9982 g/mL, $\rho_{25,b}$ (the density of buffer at 25 °C) is 1.001132 g/mL, $\eta_{20,w}$ (the viscosity of water at 20 °C) is 0.01002 P, and $\eta_{25,b}$ is 0.00905 P.

Cross-Linking of Primase on DNA. Primase was N-terminally labeled with biotin by incubating the protein [in 20 mM HEPES (pH 7.0), 150 mM NaCl, 10% glycerol] with 5 molar equiv of *d*-biotin succinimide (Molecular Probes) for 14 h at 4 °C. Excess biotin was removed by subjecting the mixture to a 1 mL Sephadex G-25 column. The biotinylated primase was cross-linked with the thiol−thiol cross-linker 1,6-bismaleimidohexane (BMH) (Pierce) on oligonucleotides of 8, 20, 24, or 45 nucleotides (Table 2). The protein (1 μM final) was mixed with oligonucelotide (0.3 μM final) to give a reaction volume of 19 μL. Cross-linking was initiated after incubating the protein and DNA for 10 min by the addition of 1 μL of BMH (20 μM final) dissolved in DMF. The reaction was quenched after 8 min by the addition of 5 μL of gel loading buffer [150 mM Tris (pH 6.8), 4% sodium dodecyl sulfate, 0.1% bromophenol blue, 14.3 mM β-mercaptoethanol, 30% glycerol]. The products were analyzed by SDS−PAGE followed by a western blot procedure using streptavidin as a probe, as described elsewhere (*30*).

Biotinylated primase was alternatively cross-linked with tris(2,2′-bipyridyl)dichlororuthenium(II) hexahydrate [Ru(II)-bpy$_3^{2+}$] (Aldrich), a photoactivatable cross-linker (*31*). Primase (1 μM final) was mixed with either the 8, 20, 24, or 45 base oligonucleotide (0.3 μM final) used in the BMH experiments in a reaction volume of 16 μL. To the mixture was added 2 μL of a 2.5 mM ammonium persulfate solution and 2 μL of a 1.5 mM Ru(II)bpy$_3^{2+}$ solution (dissolved in H_2O) in the dark. Cross-linking was performed by exposure to a 60 W desk lamp for 2 s. Immediately thereafter, 5 μL of gel loading buffer was added and the cross-linked protein separated by SDS−PAGE followed by a western blot procedure to visualize the biotin label.

RESULTS

Primase Cloning, Purification, and Characterization. The primase was first isolated in 1985 from T4 phage-infected cells or from a plasmid-based expression system (*32*, *33*). In the current work, the primase was expressed as an intein fusion with a chitin binding domain, which was separated from other cellular proteins on a chitin column, and the primase was liberated by cleavage with β-ME. This procedure affords native untagged protein. Purification on a phosphocellulose column through a salt gradient yielded protein that was >98% pure as judged by densitometry of an SDS−PAGE gel. Some typical gels from a primase purification are included in the Supporting Information (Figure S1). The cleavage yield was greatly increased by the substitution of glycine for isoleucine at the primase C-terminus. This I342G primase was identical to the wild-type sequence in activity and binding of zinc and ssDNA, and was employed in all of the following experiments. Typically 60−75 mg of purified primase could be obtained from 150 g of frozen cells, corresponding to 3 L of liquid culture. The primase protein was determined by atomic absorption to contain 0.8−1 equiv of zinc for several different preparations.

Determination of free thiol by DTNB titration provided evidence for one readily accessible (quickly titrated) and one less-accessible free cysteine. The latter titrated over 30 min at room temperature. In the presence of DNA, however, 2 equiv of thiol titrated quickly, suggesting that the less-exposed residue becomes more exposed upon DNA binding. The primase protein has six cysteines, and four of them (Cys37, Cys40, Cys65, and Cys68) are expected to coordinate to the zinc ion, so this result suggests that in the free primase one of the two remaining cysteines (Cys124 or Cys144) is exposed while the other is relatively buried but becomes available through a primase conformational change upon binding DNA.

Labeling of the primase with a fluorescent cysteine-reactive probe followed by trypsin cleavage, isolation of the fluorescent fragment by HPLC, and mass spectrometry to determine the site of label revealed that Cys144 was the only solvent-accessible free cysteine residue (data not shown) in the absence of DNA. However, labeling of the protein with thiol-reactive probes in the presence of DNA results in labeling of two cysteine residues, Cys144 and Cys124, with Cys124 being predominantly labeled (data not shown).

Priming Activity. Primase activity was determined by monitoring the synthesis of radiolabeled pentaribonucleotides

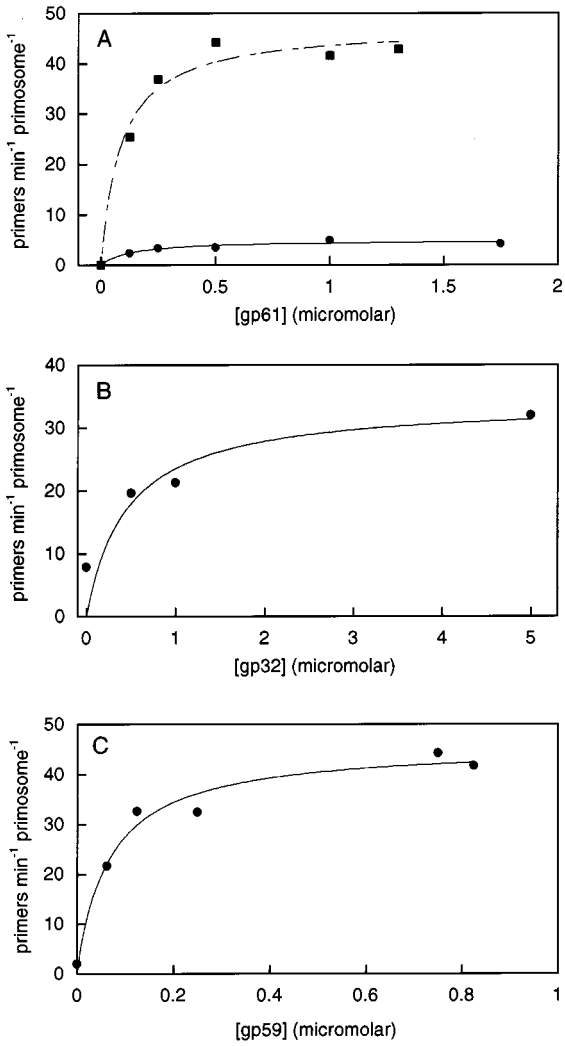

FIGURE 2: Effect of various proteins on primer formation. Assay conditions were as described under Experimental Procedures. Concentrations were as follows unless specified otherwise: 125 nM helicase hexamers, 750 nM primase, 1 mM rNTPs, 4 mM additional ATP, and 1.4 μM priming sites on M13mp18. (A) Effect of primase on primer formation in the absence (circles and solid line) and presence (squares and dashed line) of 5 μM gp32 and 750 nM gp59. In the absence of gp32 and gp59, the maximum turnover number was 4.9 ± 0.4 min^{-1}, and the K_d was 130 ± 45 nM. In the presence of those proteins, the maximum turnover number was 47 ± 3 min^{-1}, and the K_d was 87 ± 25 nM. (B) Effect of gp32 on primer formation in the presence of 750 nM gp59. The fit yields a maximum turnover number of 34 ± 8 primers min^{-1} primosome^{-1} and a K_d of 450 ± 40 nM. (C) Effect of gp59 on primer formation in the presence of 5 μM gp32. The fit yields a maximum turnover number of 46 ± 3 primers min^{-1} primosome^{-1} and a K_d of 67 ± 16 nM.

which were separated from the reaction solution by denaturing PAGE. Primer synthesis as a function of primase concentration at constant helicase concentration in the absence of single-stranded DNA binding protein (gp32) and helicase accessory factor (gp59) is shown in Figure 2A (circles). In their absence, the K_d for primase was 130 ± 45 nM and the V_{max} was 4.9 ± 0.4 min^{-1}. Inclusion of gp59 so that this protein was stoichiometric with helicase monomers and titration with gp32 resulted in the outcome shown in Figure 2B. The K_d for gp32 was 450 ± 40 nM, and the V_{max} was 34 ± 8 min^{-1}. The binding of gp32 to ssDNA is highly cooperative and salt-dependent, and occurs with an apparent binding constant determined by fluorescence titrations of

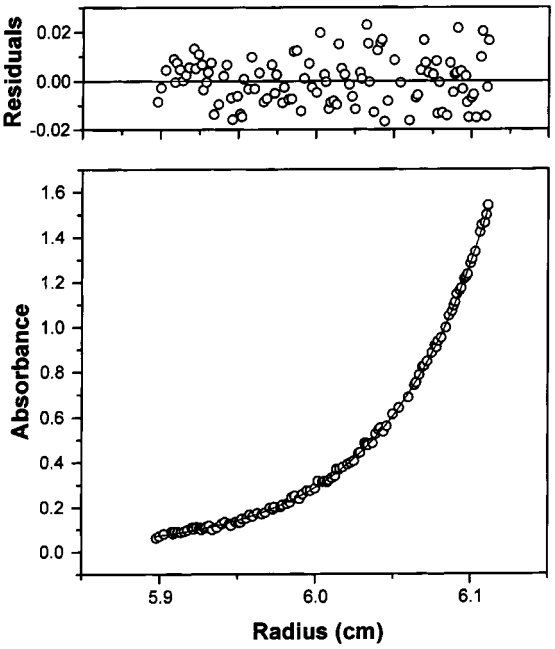

FIGURE 3: Sedimentation equilibrium data showing the primase in the absence of DNA at 18 000 rpm. The fit shown is to a single-species model, and the molecular weight determined from these data is 39 750 ± 130.

250−500 nM (*34*). Considering its site size of ~8 bases (*34*−*37*), 5 μM gp32 represents 100% coverage of the single-stranded DNA. Further addition of gp32 did not result in additional rate increases. The effect of varying concentrations of gp59 in the presence of 5 μM gp32 is shown in Figure 2C. The K_d for gp59 was 67 ± 16 nM, and the V_{max} was 46 ± 3 min^{-1}. The apparent K_d is slightly less than the range (from 140 nM to 1.5 μM) previously reported (*38*). The binding of gp59 (site size 9 bases) to ssDNA, like that of gp32 to ssDNA, is cooperative and salt-dependent. Full activation was seen at approximately 400 nM gp59 when the helicase concentration was 750 nM (monomers). In Figure 2A, the effect of varying primase in the presence of 750 nM gp59 and 5 μM gp32 is depicted (squares). With these protein factors, the K_d for primase was 87 ± 25 nM, and the V_{max} was 47 ± 3 min^{-1}. The same experiment was carried out at 150 nM helicase monomers (Figure S3), and maximal activation was again observed at approximately one primase per helicase monomer. The measured K_d was thus within error of the value determined in the absence of these proteins, but the maximum turnover was 10-fold faster. Increasing the ribonucleotide or template DNA concentration afforded only modest increases over the rates shown in Figure 2A. The maximum measured rate in any experiment was 60 min^{-1}, or one primer per second per primosome.

Primer formation could also be monitored by using short oligonucleotides as templates in place of single-stranded M13mp18 DNA. The oligonucleotide length dependence of this priming is presented in Table 2. The primase activity on these oligos was quite low (~0.2 primer min^{-1} primosome^{-1}) and was not observed for oligos except the 45mer.

Protein−Protein Interactions. (A) No Primase Self-Association by Analytical Ultracentrifugation. A typical result for sedimentation equilibrium (Figure 3) and a compilation of the results for sedimentation velocity (Figure 4) are shown. The apparent molecular weight in the former experiment was

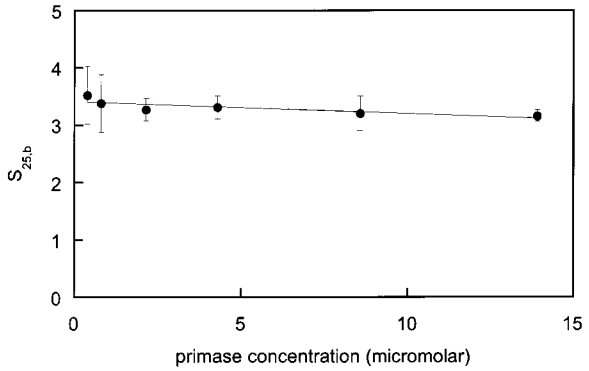

FIGURE 4: Sedimentation velocity data showing the primase at a range of concentrations. The sedimentation coefficient ($s°_{25,b}$) at infinite dilution is 3.41.

39 750 ± 130, which agrees with the monomer molecular weight. No evidence of dimer formation was seen. The calculated $s^o_{25,b}$ sedimentation coefficient of 3.41 S corresponded to an $s^o_{20,w}$ of 3.23 S. The theoretical maximum for a monomer is 3.6457, and for a dimer, 5.7873. Taken together, these data suggest, in agreement with earlier experiments (*39*), that the primase does not self-associate in solution in the absence of DNA. These experiments were performed in two different buffers, in potassium phosphate and in a Tris complex buffer used for activity assays and ITC, and no evidence of primase self-association was observed in either case. Attempts to repeat these experiments in the presence of DNA failed due to protein precipitation at the relatively high concentrations and long times required for the experiment.

(B) Primase−Helicase Binding by ITC. The interaction between primase and helicase in the presence of single-stranded DNA is shown in Figure 5. Evidence of binding could be seen in the absence of DNA, but the binding was at least 10-fold weaker (data not shown). The binding required ATP or ATP-γ-S; in the absence of nucleotides, no binding was observed. Including ATP caused a large background heat of ATP hydrolysis which resulted in poor and irreproducible fits. The stoichiometry (0.86 primase molecule per helicase monomer) is different from the value determined by quantitation of proteins in a bandshift (*39*).

(C) Primase−gp32 Binding by ITC. The binding of primase to gp32 has been reported (*33*). Isothermal titration calorimetry was employed to characterize this binding, with a typical result shown in Figure 6. The binding is exothermic by 10 kcal/mol, and a fit to a one-site model yields a K_d of 860 ± 370 nM for the dissociation of the gp32/gp61 complex. At the gp32 concentration in the ITC cell, this protein probably exists as a dimer, although the fit was performed using the monomer concentration and returns a value of one primase binding to four gp32 monomers, or to two gp32 dimers.

Protein−DNA Interactions. (A) Primase Binding to ssDNA by ITC. The result of titrating 45mer ssDNA containing a priming site into the primase protein is shown in Figure S4. At 25 °C, the binding was tight (K_d ~ 50 nM) and endothermic and proceeded with a stoichiometry of 3−4 primase molecules per ssDNA. With this experimental design, the primase is at high concentration in the cell to which DNA is added, but additional binding phases suggested by the data were not well resolved (Figure S4).

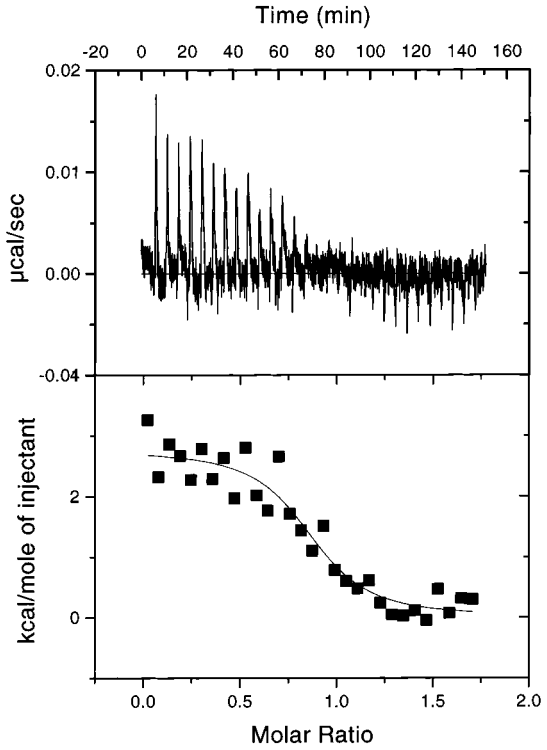

FIGURE 5: Isothermal titration calorimetry study of primase binding to helicase at 25 °C. A 53.3 μM solution of primase was titrated in 5 μL increments into a solution of 3.35 μM helicase monomers and 600 nM 45mer ssDNA. Each solution contained 1 mM ATP-γ-S. The fit shown is to a one-site model and returns the parameters $N = 0.86 \pm 0.03$, $K_d = 100 \pm 40$ nM, $\Delta H = 2.8 \pm 0.1$ kcal/mol, and $\Delta S = 41$ cal/(mol·K).

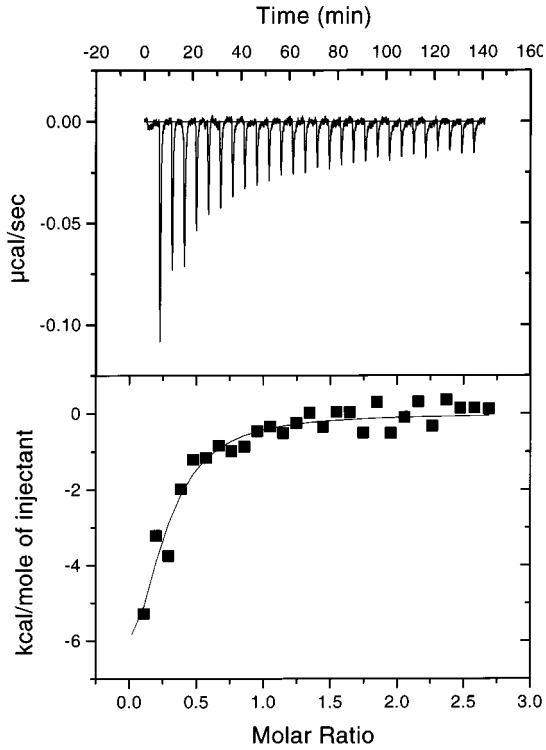

FIGURE 6: Isothermal titration calorimetry study of primase binding to the single-stranded DNA binding protein, gp 32, at 25 °C. A 65 μM solution of primase was titrated in 10 μL increments into a 5 μM solution of gp32. The fit shown is to a one-site model and returns the parameters $N = 0.22 \pm 0.08$, $K_d = 860 \pm 370$ nM, $\Delta H = -10.5 \pm 4$ kcal/mol, and $\Delta S = -7.42$ cal/(mol·K).

Oligonucleotides of varying lengths containing a priming site were also employed in these titrations, and the results are shown in Table 2. For oligos shorter than a 20mer, no binding was observed. Weak binding was observed for a 22mer, and binding parameters and stoichiometry for the 24mer and 45mer were quite similar. We noticed but did not explore a dependence on DNA sequence flanking the priming site in these binding reactions. For example, primase will bind avidly to the 24mer in Table 2, but no binding is detected to a 24mer which is poly(dT) with a single G in the middle to produce a 5′-GTT-3′ priming site (data not shown).

The reverse titration (Figures S5 and S6), injecting primase protein into a solution of ssDNA, resulted in better-resolved binding phases. The results of this experiment, performed as a function of temperature, are presented in Figure S5. As many as three binding phases were required to fit the data at some temperatures, for example at 30 and 33 °C. Better fits were obtained when binding cooperativity was included in the model, but the errors were quite large when fitting the data to so many variables. The K_d values obtained from these fits were not considered meaningful. In general, binding became more endothermic and tighter as temperature increased to the physiologically relevant value of 37 °C.

The presence of Mg^{2+} is required for tight primase−DNA binding. If this divalent metal was omitted from the complex buffer and the ionic strength compensated by additional sodium acetate, only very weak binding was observed (Figure S7). In the X-ray crystal structures of the *E. coli* primase catalytic domain, Mg^{2+} ions have been located in the putative DNA binding crevice (*13*, *14*). Other divalent cations were not tested.

The binding of primase to DNA in the presence and absence of a priming site is addressed by the data in Figure S6. Trace a shows binding to an oligo containing a primase recognition site, while trace b shows binding to an oligo which does not contain a such a site. Binding to the oligo with the priming site is tighter, though nonspecific binding is also observed. Some priming, weak compared to that on an oligo containing a priming site, was observed on the oligo not containing a canonical 5′-GTT-3′ or 5′-GCT-3′ priming site (data not shown).

(B) Cross-Linking Studies of Primase on DNA. Primase was N-terminally labeled with a biotin probe and cross-linked in the presence of oligonucleotides of either 8, 20, 24, or 45 bases. This biotinylation allows detection at very low protein concentrations so that nonspecific association is minimized (*30*).

Cross-linking of biotinylated primase with Ru(II)bpy_3^{2+}, a sensitive, zero-length cross-linker, indicated that the protein was capable of self-associating on DNA. Ru(II)bpy_3^{2+} is a photoactivatable cross-linker that can be excited with visible light and is believed to cross-link tyrosine residues through generation of a tyrosine radical intermediate (*31*). Irradiated in the absence of Ru(II)bpy_3^{2+}, or in the presence of Ru(II)-bpy_3^{2+} but absence of DNA, primase migrates as a monomer when subjected to SDS−PAGE followed by a western blot procedure to visualize the biotin label (Figure 7A). However, in the presence of both cross-linker and DNA, a band corresponding to a primase cross-link is visualized with a molecular mass of approximately 120 kDa, which is consistent with a primase trimer. The trimer is observed in the presence of all oligonucleotides, even the 8mer. The ratio

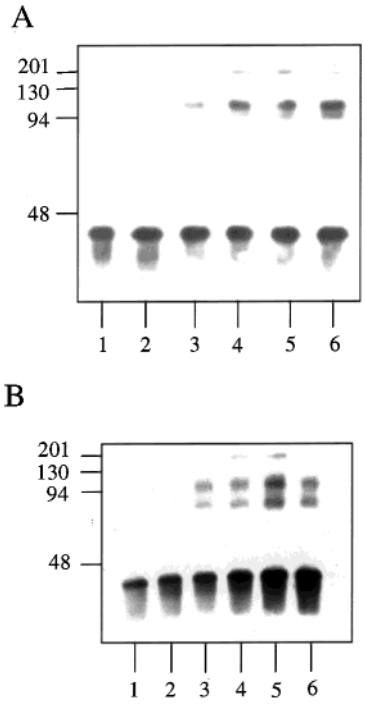

FIGURE 7: Cross-linking of primase. Primase was cross-linked with tris(2,2′-bipyridyl)dichlororuthenium(II) hexahydrate (panel A) or 1,6-bis-maleimidohexane (panel B) in the presence or absence of DNA. The products of the reaction were separated by SDS−PAGE, blotted onto nitrocellulose, and detected with streptavidin−horseradish peroxidase (*30*). Lanes 1−6 in each panel depict the following: (1) gp61, (2) gp61 in the presence of cross-linker, (3) gp61 plus an 8 base oligonucleotide and cross-linker, (4) gp61 plus a 20 base oligonucleotide and cross-linker, (5) gp61 plus a 24 base oligonucleotide and cross-linker, (6) gp61 in the presence of a 45 base oligonucleotide and cross-linker.

of protein and DNA was varied in these experiments (data not shown). The predominant cross-linked products were trimers in all cases, although some higher molecular weight products could be seen on the longer oligonucleotides at higher protein concentrations.

Cross-linking of the biotinylated primase with BMH, a thiol−thiol cross-linker with a 16 Å linker length, yielded similar results. In the absence of cross-linker or DNA, primase is monomeric (Figure 7B). In the presence of BMH and oligonucleotide, cross-links are observed that migrate with masses of 80 and 120 kDa, corresponding to a primase dimer and trimer, respectively. The intensity of the cross-linked bands is lower in the presence of the 8 or 20 base oligonucleotide relative to the longer oligonucleotides, indicating that the complexes formed on the shorter DNA may be more transient.

DISCUSSION

Priming Activity. The activity of the primase is most often measured indirectly by its ability to support primer-dependent lagging strand DNA synthesis (*40*). When primer synthesis has been measured directly with T4 proteins on a single-stranded DNA template, however, the measured turnover numbers [∼1 primer per minute per primosome (*9*, *22*, *41*)] have been slower than is necessary to support in vivo DNA replication. This process occurs with the replisome at a rate of 520−750 bp/s (*42*). Okazaki fragment lengths are on the order of 2000 bases (*43*), so a primer must be made on the unwinding exposed DNA at least every once every 4 s or ∼15 primers min^{-1} $primosome^{-1}$.

A similar slow rate of priming to that in T4 has been measured for the *E. coli* proteins [∼1 primer min^{-1} $primosome^{-1}$ (*44*)]. For bacteriophage T7, a much simpler system comprising fewer protein factors and with the primase and helicase activities condensed into a single protein, the measured rates of primer synthesis are much faster [∼2 primers s^{-1} $primosome^{-1}$ (*45*)]. Clearly, the chemistry of oligoribonucleotide formation is not rate-limiting. We considered that the slow rate reported in the T4 literature and measured in the presence of primase and helicase proteins alone (Figure 2A) might be due to slow or improper loading of these primosome proteins onto the ssDNA. In the absence of other protein factors, the maximum rate of primer synthesis was about one primer every 12 s (Figure 2A). Including optimal levels of gp32 and gp59, however, while not affording a measurably tighter complex as expressed by the primase affinity for ssDNA, did increase the priming rate to almost 1 primer per second per primosome (V_{max} = 50 min^{-1}), sufficient for the in vivo operation of the replisome.

An analysis of the effect on primer synthesis (when the primase:helicase monomer ratio is 1:1) of varying the concentrations of gp32 and gp59 is shown in Figure 2B,C. At a 1:1 gp59:gp41 (monomers) ratio, the rate increases with increasing gp32 concentration, reaching a plateau at 100% coverage of the available single-stranded DNA assuming a gp32 site size of 8 bases (*34*). At this level of gp32 but varying the gp59 concentration, the rate increased to a maximum at a gp59 level that was less than the helicase monomer (ratio of ∼1:2; gp59:gp41 monomer). While the helicase does not require gp59 for processivity (*46*), the two proteins can form a 1:1 complex (*47*) which stimulates the helicase unwinding activity. What these new data suggest is that, on the circular ssDNA system described here, gp59 can act catalytically to "load" the primosome.

Oligomeric State of the Primase. The kinetic data are consistent with an active primosome featuring one helicase unit (six monomers) complexed with six primases. These data call into question the native state of the primase. In earlier work, the primase did not form intermolecular cross-links, even in the presence of nucleotide cofactor, in the absence of DNA or other proteins (*39*). This result suggests that the protein remains a monomer under these conditions. In the current work, analytical ultracentrifugation was used in addition to cross-linking to characterize the oligomerization state of the primase in the absence of DNA or protein cofactors. Both equilibrium and velocity measurements support the previous result (*39*) that the primase remains a monomer. Attempts to repeat these experiments in the presence of short oligonucleotides resulted in protein precipitation at the high concentrations (2.5 μM oligo, up to 15 μM protein) and long times necessary to complete the experiment. This aggregation was also noted in the previous report (*39*). Although these are similar concentrations to the ones used for ITC, no precipitation was observed in those experiments. We postulate that the slow mixing of protein and DNA with stirring over the course of several hours may overcome this precipitation problem. ITC also provides additional evidence that the primase is a monomer in solution. Dilution control experiments with the primase did not show evidence of a monomer−oligomer equilibrium.

Protein−Protein Interactions. The stoichiometry of the primase in complex with helicase and other auxiliary proteins was determined by ITC for comparison to that obtained from the kinetic data. ITC is an excellent technique for the detection of macromolecular interactions because it can provide accurate measures of stoichiometry, binding constant, and enthalpy and entropy of binding. The direct interaction of the untagged, unmodified molecules is monitored. In the ITC experiment, one binding partner is titrated into the other. The instrument measures the amount of power required to compensate for each injection and maintain a constant temperature with respect to a reference cell. In the convention used in this work, upward peaks (more power supplied to sample cell) describe endothermic binding, while downward peaks describe exothermic binding. As the binding sites are saturated, each injection peak becomes smaller until the heat reflects only dilution of the titrant molecule. An independent control experiment with only buffer in the cell provides a measure of this background. Each of the experiments in this paper for which data fits are given were fit to a single-site binding model. Moreover, the data are plotted as the molar ratio, not as a function of the variable component, and are obtained under conditions where the given system reaches saturation. This model does not specify stoichiometry, which is determined in the fit, but instead means that a single binding constant and enthalpy were used to describe the data.

Titrations of primase into helicase in the presence of an oligonucleotide and ATP-γ-S resulted in plots such as the one shown in Figure 5. Under these conditions, the helicase exists exclusively as a hexamer (*48*) and should be totally bound to the DNA. The K_d (100 nM) for ssDNA is very close to the value determined from fitting of the activity data in Figure 2A. Thus, the effect on activity of titrating in the primase can be rationalized entirely based on the equilibrium constant for primosome formation. The binding occurred with a ΔH of 2.8 kcal/mol and a stoichiometry of 0.9 primase molecule per helicase monomer, or nearly six per helicase hexamer.

Binding was not observed when the nucleotide analogue was omitted. When ATP was used, each injection resulted in the addition of unhydrolyzed ATP to the helicase−ssDNA mixture, and the hydrolysis of this ATP resulted in a large background heat of reaction. Binding of primase and helicase in the presence of nucleotide and the absence of oligonucleotide was barely detectable, but proceeded with a very small binding enthalpy ($\Delta H < 1$ kcal/mol). The data in Figure 5 do not come from primase−DNA binding with helicase not participating, because both the stoichiometry and the enthalpy changes are very different from those observed with primase and DNA alone (see below).

These results are in disagreement with previous publications. Two lines of evidence support the model that, as in *E. coli*, one primase and six helicase monomers form an active primosome in bacteriophage T4. Richardson and Nossal (*41*) studied the unwinding of dsDNA by helicase in the presence of increasing concentrations of primase and found that this unwinding was maximally stimulated at a ratio of five monomers of helicase per monomer of primase. Later Dong and von Hippel (*39*) reported the titration of increasing amounts of helicase into fixed concentrations of ssDNA and primase until helicase was in excess. The complexes were purified by native gel electrophoresis, isolated from the gel, and then subjected to denaturing SDS−PAGE. The amounts of primase and helicase were determined by densitometry of the resulting stained gels. The ratio was determined to be 6 (±1):1 helicase monomers to primase. The reason for the discrepancy may arise from the differing assays; in the former, one is measuring the helicase not primase activity; in the latter, one risks loss of protein units during sample manipulation.

The ratio of primase to helicase in the primosome varies among the characterized systems. In bacteriophage T7, in which the primase and helicase activities occur on the same polypeptide, formation of a helicase hexamer places six primase units in the primosome. The primase active sites must face outward because a primase−helicase hexamer encircling one DNA strand can prime effectively on a different DNA strand (*49*). In *E. coli*, the primosome has been shown to contain just one primase monomer per helicase hexamer, and the location of the primase active site with repect to the helicase is not known (*13*). In several important respects, such as the number of protein components and complexity of the system, T4 DNA replication is intermediate between T7 (which is simpler) and *E. coli* (which is more complex).

This new evidence that the primase forms at least a trimer on single-stranded DNA, and a hexamer in the presence of the helicase, has important implications for primosome function. The findings that the primase can oligomerize on a piece of single-stranded DNA as short as an 8mer, and that it associates with the helicase in a 1:1 monomer:monomer ratio, suggest that it might also form a ring. If so (as shown in Figure 1), then the single-stranded DNA would have to loop out through the ring as is the case in *E. coli* primosome (see above), where the primase active site lies on the outside of the complex. Circumscribing the DNA might also help the primase stay associated with the primosome during helicase translocation.

If the rate of binding were known, the K_d measured by ITC and determined from activity assays (50−100 nM) could be used to calculate how fast the primase dissociates from the primosome. Estimation of this k_{on}, however, is problematic. A diffusion-controlled $k_{on} = 10^6\ M^{-1}\ s^{-1}$ can be increased to as much as $10^9\ M^{-1}\ s^{-1}$ by electrostatic attraction (*50*) as might occur for a positively charged protein (the p*I* of the primase is 9.4 as calculated from the sequence by the program Sednterp) and negatively charged DNA. This variation means that the k_{off} might be as slow as $0.05\ s^{-1}$ or as fast as $100\ s^{-1}$. These equilibrium data do not, then, answer the question of whether the primase remains associated with the helicase during the replication of one copy of the T4 genome (172 kbp). If the off rate is as slow as $0.05\ s^{-1}$, then the primase will not dissociate many times, if at all, during replication. If the off rate is nearer to $100\ s^{-1}$, primase may dissociate and bind anew to make each primer, a phenomenon reported in the *E. coli* replication system not just to occur but also to control the timing of primer synthesis (*51*). Both models are consistent with the current data.

Interactions involving the primase and other proteins may also shed light on how the newly synthesized primer, which is quite labile, is handed off to the polymerase protein for extension. A direct handoff featuring a primase−polymerase interaction as is observed for bacteriophage T7 (*52*) is one possibility, but no such interaction of the T4 primase with

the polymerase has yet been detected. ITC experiments (5 μM polymerase titrated with 50 μM primase) failed to provide evidence for any interaction (data not shown). A negative result in the ITC, however, can be due to a very small ΔH of binding, so that such binding would go undetected.

Primase has previously been reported to bind gp32 as well as to single-stranded and double-stranded DNA (*33*). Primase−gp32 interactions could be part of three-point handoff of the newly synthesized primer to the polymerase, similar to the one postulated for *E. coli* (*53*). In this scenario, a molecule of gp32 displaces the primase from the newly synthesized primer and prevents the latter's dissociation. In turn, gp32 is displaced by gp44/62 as it acts to load the clamp protein to the 3′ side of the polymerase concomitant with release of the primer. The quantitation of the primase−gp32 interaction (Figure 6) provides some preliminary evidence for this sequence of events. Evidence for an interaction between gp32 and the clamp loader (gp44/62), the second part of a putative three-point handoff, has been detected by chemical cross-linking and ITC, and is a focus of current study (M. U. Mayer and S. J. Benkovic, unpublished results).

Protein−DNA Interactions. Primase binding to single-stranded DNA in the absence of helicase has been reported (*33*), and the characterization of this binding by ITC is discussed here. Some notable and immediate conclusions from the data in Figures S3−S6 are that the ratio of primase to oligo is greater than 1:1, that the net binding phenomenon is endothermic at temperatures above 25 °C, and that Mg^{2+} is required for binding. The first two points will be discussed in turn.

It is clear from the data in Figure S4, and even more evident when the position of the binding partners is reversed and the primase is titrated into the oligonucleotide (Figures S5 and S6), that greater than one primase monomer can bind to each oligo. A study of the oligo length dependence of this phenomenon (Table 2) shows that, for all oligos on which binding can be detected, three to four primase molecules bind. This effect is not what one would expect if, like gp32, primase could coat the DNA in a non-sequence-specific manner. In that case, if the 24mer bound three molecules of the primase, then the 45mer should bind six. It does not. Instead, the result suggests that, once the oligo reaches a critical length of 22−24 nucleotides, 3 or 4 primase molecules cluster around the priming site, and long stretches of DNA on either side do not result in further or significantly tighter binding. Transient primase binding, predominantly as a protein trimer, to even shorter oligos has been detected by cross-linking, and will be discussed below.

The ability of the primosome to make pentaribonucleotides on these short oligos was also investigated (Table 2). Although the primase alone will bind to a 22mer and a 24mer, no primer synthesis was detected on those oligos. This result suggests that primase binding is necessary but not sufficient for primer formation. The primase alone carries out only very inefficient primer synthesis, and the helicase greatly stimulates this synthesis (*54, 55*). The binding site size of the helicase is 12−20 nucleotides (*56*). Therefore, the 24mer is probably too short for both the primase and helicase to bind, and so priming is inefficient and not observed.

The temperature dependence of primase−ssDNA binding is depicted in Figure S5. The net effect is exothermic for temperatures at and below 25 °C. Above this temperature, the binding is predominantly endothermic. Extensive attempts were made to find unique fits for these data. Three sequential binding sites were required to fit the data, but because each of these incorporates several variables (even with fixed stoichiometry, K and ΔH can vary), the resulting fit parameters carried uncertainties greater than the values themselves.

Binding events usually proceed with a decrease in entropy. In the simplest case, two free molecules become one complex, with a corresponding loss in disorder. Therefore, if thermodynamically favored, such a binding event will be exothermic. It is important to remember, though, that the ITC measures a composite phenomenon. As two molecules bind, the loss in entropy can be offset by conformational changes or by release of water or counterions. In some cases, as in this one, there is a net gain in entropy, and binding may be endothermic. Protein−ssDNA binding reactions, explored in great detail by Lohman and co-workers for single-stranded binding proteins and oligonucleotides, can be some of the most exothermic macromolecular interactions (*57*). The enthalpy changes are salt- and sequence-dependent, and come mainly from aromatic amino acids stacking with DNA bases upon binding and with bases unstacking one from another. Under conditions where the latter is favored, endothermic binding has been observed (*58*).

Primase binding to an oligonucleotide with or without a priming site was investigated, and some typical results are shown in Figure S6. While the primase bound more tightly to the oligo containing the priming site, there was significant nonspecific binding to the oligo which did not contain such a site. This result agrees with cross-linking data, which show that multimers of the primase form on the latter 45mer oligos (data not shown). In *E. coli*, it has been reported that the helicase affects the base specificity of the primase (*59*). We have shown above that primase binding to an oligo is necessary but not sufficient for priming. Also, there is a low level of nonspecific primer formation on oligos not containing a canonical priming site. It could well be that, in T4, the helicase is necessary for the sequence-specific recognition event that results in efficient synthesis of a primer.

Cross-Linking of Primase on DNA. Cross-linking experiments using the photoactivatable cross-linker $Ru(II)bpy_3^{2+}$ or the thiol−thiol cross-linker BMH indicated that the primase forms primarily trimers on oligonucleotides ranging in size from 8 bases to 45 bases, thus corroborating the ITC data. The protein appeared to form distinct complexes instead of merely coating the DNA since the same oligomeric state was observed for all oligonucleotides used. However, the yield of cross-linking was highest in the presence of the 24 or 45 base oligonucleotides, suggesting that association of the proteins is strongest on DNA longer than 20 bases.

Since trimeric cross-linked proteins were seen in the presence of BMH, at least two different cysteine residues must be involved. Primase contains six cysteine residues; four are involved in ligation of the zinc ion. Apparently, binding to DNA induces a conformational change in the protein that exposes Cys124 (see above) and also allows self-association. When this happens, both cysteine residues, Cys124 and Cys144, are in close proximity to the subunit

interface(s) and can be cross-linked by the 16 Å BMH cross-linker to give the trimeric species observed.

CONCLUSION

In this paper, we report a physiologically competent priming rate approaching 1 primer s^{-1} primosome^{-1}, a rate which requires a catalytic amount of the gp59 helicase loading factor and sufficient gp32 single-stranded DNA binding protein to coat the DNA template. The interactions of the primase with gp32 and with the helicase in the presence of DNA and a nucleotide analogue have been characterized by ITC. Notably, the primase and helicase can interact with a stoichiometry of one primase per helicase monomer. Stable primase−ssDNA binding requires an oligo of at least 22 nucleotides, although transient binding can be detected by chemical cross-linking on oligos as short as 8 nucleotides. Primase binds to single-stranded DNA primarily as a trimer. Cysteine labeling experiments support DNA binding-induced conformational changes in the primase protein. The results suggest that, of the two free cysteines in the protein, one becomes significantly more exposed upon DNA binding. Priming on a single-stranded template requires more than 24 bases, most likely because of the binding site requirements of the helicase.

ACKNOWLEDGMENT

We gratefully acknowledge Mr. Mark Signs for assistance with the fermentation, Dr. Henry Gong for assistance with the atomic absorption measurements, and Dr. Stephen Alley, Dr. Frank Salinas, and Dr. M. Uljana Mayer for materials and helpful discussions.

SUPPORTING INFORMATION AVAILABLE

Seven figures showing SDS−PAGE analysis of a typical primase purification, denaturing PAGE analysis of a primase assay, effect of primase concentration on the rate of primer formation at low helicase concentrations, and ITC studies of primase binding to ssDNA (10 pages). This material is available free of charge via the Internet at http://pubs.acs.org.

REFERENCES

1. Benkovic, S. J., Valentine, A. M., and Salinas, F. (2001) *Annu. Rev. Biochem. 70*, 181−208.
2. Nossal, N. G. (1994) in *Molecular Biology of Bacteriophage T4* (Karam, J. D., Ed.) pp 43−53, American Society for Microbiology, Washington, DC.
3. Sexton, D. J., Berdis, A. J., and Benkovic, S. J. (1997) *Curr. Opin. Chem. Biol. 1*, 316−322.
4. Pan, H., and Wigley, D. B. (2000) *Struct. Fold. Des. 8*, 231−239.
5. Qian, X., Gozani, S. N., Yoon, H., Jeon, C. J., Agarwal, K., and Weiss, M. A. (1993) *Biochemistry 32*, 9944−9959.
6. Qian, X., Jeon, C., Yoon, H., Agarwal, K., and Weiss, M. A. (1993) *Nature 365*, 277−279.
7. Zhu, W., Zeng, Q., Colangelo, C. M., Lewis, M., Summers, M. F., and Scott, R. A. (1996) *Nat. Struct. Biol. 3*, 122−124.
8. Wang, B., Jones, D. N., Kaine, B. P., and Weiss, M. A. (1998) *Structure 6*, 555−569.
9. Nossal, N. G. (1980) *J. Biol. Chem. 255*, 2176−2182.
10. Liu, C. C., and Alberts, B. M. (1980) *Proc. Natl. Acad. Sci. U.S.A. 77*, 5698−5702.
11. Griep, M. A. (1995) *Indian J. Biochem. Biophys. 32*, 171−178.
12. Kusakabe, T., and Richardson, C. C. (1996) *J. Biol. Chem. 271*, 19563−19570.
13. Keck, J. L., Roche, D. D., Lynch, A. S., and Berger, J. M. (2000) *Science 287*, 2482−2486.
14. Podobnik, M., McInerney, P., O'Donnell, M., and Kuriyan, J. (2000) *J. Mol. Biol. 300*, 353−362.
15. Leipe, D. D., Aravind, L., and Koonin, E. V. (1999) *Nucleic Acids Res. 27*, 3389−3401.
16. Aravind, L., Leipe, D. D., and Koonin, E. V. (1998) *Nucleic Acids Res. 26*, 4205−4213.
17. Huber, R., Kaiser, J. T., and Augustin, M. A. (2001) *Nat. Struct. Biol. 8*, 57−61.
18. Jing, D. H., Dong, F., Latham, G. J., and von Hippel, P. H. (1999) *J. Biol. Chem. 274*, 27287−27298.
19. Shier, V. K., Hancey, C. J., and Benkovic, S. J. (2001) *J. Biol. Chem. 276*, 14744−14751.
20. Pace, C. N., Vajdos, F., Fee, L., Grimsley, G., and Gray, T. (1995) *Protein Sci. 4*, 2411−2423.
21. Riddles, P. W., Blakeley, R. L., and Zerner, B. (1983) *Methods Enzymol. 91*, 49−60.
22. Berdis, A. J., and Benkovic, S. J. (1998) *Proc. Natl. Acad. Sci. U.S.A. 95*, 11128−11133.
23. Shieh, B., Su, I. J., Chuang, W. J., and Li, C. (1998) *BioTechniques 24*, 60−64.
24. Sambrook, J., Fritsch, E. F., and Maniatis, T. (1989) *Molecular Cloning: A Laboratory Manual*, 2nd ed., Cold Spring Harbor Laboratory Press, Cold Spring Harbor, NY.
25. Fisher, H. F., and Singh, N. (1995) *Methods Enzymol. 259*, 194−221.
26. Ladbury, J. E., and Chowdhry, B. Z. (1996) *Chem. Biol. 3*, 791−801.
27. Doyle, M. L. (1997) *Curr. Opin. Biotechnol. 8*, 31−35.
28. Pierce, M. M., Raman, C. S., and Nall, B. T. (1999) *Methods 19*, 213−221.
29. Holdgate, G. A. (2001) *BioTechniques 31*, 164−184.
30. Alley, S. C., Ishmael, F. T., Jones, A. D., and Benkovic, S. J. (2000) *J. Am. Chem. Soc. 122*, 6126−6127.
31. Fancy, D. A., and Kodadek, T. (1999) *Proc. Natl. Acad. Sci. U.S.A. 96*, 6020−6024.
32. Hinton, D. M., and Nossal, N. G. (1985) *J. Biol. Chem. 260*, 12858−12865.
33. Burke, R. L., Munn, M., Barry, J., and Alberts, B. M. (1985) *J. Biol. Chem. 260*, 1711−1722.
34. Villemain, J. L., and Giedroc, D. P. (1993) *Biochemistry 32*, 11235−11246.
35. Kowalczykowski, S. C., Lonberg, N., Newport, J. W., Paul, L. S., and von Hippel, P. H. (1980) *Biophys. J. 32*, 403−418.
36. Scheerhagen, M. A., Vlaanderen, C. A., Blok, J., and van Grondelle, R. (1986) *J. Biomol. Struct. Dyn. 3*, 887−898.
37. Shamoo, Y., Friedman, A. M., Parsons, M. R., Konigsberg, W. H., and Steitz, T. A. (1995) *Nature 376*, 362−366.
38. Lefebvre, S. D., and Morrical, S. W. (1997) *J. Mol. Biol. 272*, 312−326.
39. Dong, F., and von Hippel, P. H. (1996) *J. Biol. Chem. 271*, 19625−19631.
40. Mendelman, L. V. (1995) *Methods Enzymol. 262*, 405−414.
41. Richardson, R. W., and Nossal, N. G. (1989) *J. Biol. Chem. 264*, 4725−4731.
42. McCarthy, D., Minner, C., Bernstein, H., and Bernstein, C. (1976) *J. Mol. Biol. 106*, 963−981.
43. Okazaki, R., Okazaki, T., Sakabe, K., Sugimoto, K., and Sugino, A. (1968) *Proc. Natl. Acad. Sci. U.S.A. 59*, 598−605.
44. Johnson, S. K., Bhattacharyya, S., and Griep, M. A. (2000) *Biochemistry 39*, 736−744.
45. Frick, D. N., and Richardson, C. C. (1999) *J. Biol. Chem. 274*, 35889−35898.
46. Schrock, R. D., and Alberts, B. (1996) *J. Biol. Chem. 271*, 16678−16682.
47. Raney, K. D., Carver, T. E., and Benkovic, S. J. (1996) *J. Biol. Chem. 271*, 14074−14081.
48. Dong, F., Gogol, E. P., and von Hippel, P. H. (1995) *J. Biol. Chem. 270*, 7462−7473.

49. Kusakabe, T., Baradaran, K., Lee, J., and Richardson, C. C. (1998) *EMBO J. 17*, 1542−1552.
50. Schreiber, G., and Fersht, A. R. (1996) *Nat. Struct. Biol. 3*, 427−431.
51. Tougu, K., and Marians, K. J. (1996) *J. Biol. Chem. 271*, 21398−21405.
52. Kato, M., Frick, D. N., Lee, J., Tabor, S., Richardson, C. C., and Ellenberger, T. (2001) *J. Biol. Chem. 28*, 28.
53. Yuzhakov, A., Kelman, Z., and O'Donnell, M. (1999) *Cell 96*, 153−163.
54. Hinton, D. M., and Nossal, N. G. (1987) *J. Biol. Chem. 262*, 10873−10878.
55. Nossal, N. G., and Hinton, D. M. (1987) *J. Biol. Chem. 262*, 10879−10885.
56. Young, M. C., Schultz, D. E., Ring, D., and von Hippel, P. H. (1994) *J. Mol. Biol. 235*, 1447−1458.
57. Kozlov, A. G., and Lohman, T. M. (1998) *J. Mol. Biol. 278*, 999−1014.
58. Kozlov, A. G., and Lohman, T. M. (1999) *Biochemistry 38*, 7388−7397.
59. Bhattacharyya, S., and Griep, M. A. (2000) *Biochemistry 39*, 745−752.

BI0108554